A Study on Correlation Between Pressure Variations and Augmentation of Heat Transfer in Acoustic Fields

Yool Kwon Oh*
Department of Mechatronics Engineering, Chosun University, 375 Seosuk-dong, Dong-gu, Gwangju 501-759, Korea
Ho Dong Yang
Department of Precision Mechanical Engineering, Chosun University, 375 Seosuk-dong, Dong-gu, Gwangju 501-759, Korea

The present paper investigated the correlation between the acoustic pressure variations and the augmentation of heat transfer in the ultrasonic induced acoustic fields. The augmentation ratios of heat transfer coefficient were experimentally measured and were compared with the profile of the pressure distribution in the acoustic fields predicted by numerical analysis. For numerical analysis, a coupled finite element-boundary element method (coupled FE-BEM) was applied. The results of the present study reveal that the acoustic pressure is higher near two ultrasonic transducers than other points where no ultrasonic transducer was installed. The augmentation trend of heat transfer is similar with the profile of the acoustic pressure distribution. In other words, as the acoustic pressure increases, the higher augmentation ratio of heat transfer is obtained. Numerical and experimental studies clearly show that the acoustic pressure variations are closely related to the augmentation of heat transfer in the acoustic fields.

Key Words : Acoustic Pressure, A Coupled FE-BEM, Ultrasonic Vibrations, Acoustic Fields, Acoustic Streaming, Ultrasonic Wave, Wave Speed

Nomenclature

c : Wave speed [m/s]
h : Heat transfer coefficient [W/(m^2·K)]
Δh : Augmentation ratio of heat transfer coefficient
g : Gravitational acceleration [m/s^2]
k_T : Compressibility
p : Pressure [Pa]
q″ : Heat flux [W/m^2]
E : Bulk modulus [N/m^2]
H : Height of solid paraffin (characteristic height)
K : Thermal conductivity of liquid phase [W/(m·K)]
Nu : Nusselt number (defined as $q''H/(K(T_h-T_f))$)
Pr : Prandtl number (defined as ν/α)
Ra* : Modified Rayleigh number (defined as $g\beta q''H^4 Pr/(K\cdot\nu^2)$)
T : Temperature [K]
X : Dimensionless horizontal position
Y : Dimensionless vertical position

Greeks

α : Thermal diffusivity of liquid phase
β : Thermal expansion coefficient
λ : Wavelength [mm]
ρ : Density of liquid paraffin
ν : Kinematic viscosity

Subscript

avg : Average
h : Heater surface
∞ : Selected location
o : Without ultrasonic vibration

* Corresponding Author,
E-mail : ygoh@mail.chosun.ac.kr
TEL : +82-62-230-7014; **FAX** : +82-62-230-7014
Department of Mechatronics Engineering, Chosun University, 375 Seosuk-dong, Dong-gu, Gwangju 501-759, Korea. (Manuscript **Received** July 29, 2003; **Revised** May 31, 2004)

1. Introduction

In resent years, the industrial applications of solid-liquid phase change have attracted considerable attention in the process of melting or solidification in enclosures. For examples, it includes metallurgical process such as casting and welding, material science applications such as crystal growth. Also, the thermal energy storage system using a latent heat of phase change material is actively applied because of all increased exploit of the solar energy and midnight electricity. Therefore, the effective augmentation technique of phase-change heat transfer is now required due to the practical importance of this subject. However, most studies have been performed on the coupled problem of phase change with natural convection in the melt layer. Only a few papers (Lemlich, 1955 ; Larson and London, 1962 ; Topp and Eisenklan, 1972 ; Fsairbanks, 1979 ; West and Taylor, 1952) dealt with the effect of ultrasonic vibrations during the melting process. In recent years, several researchers (Iida et al., 1991 ; Frenkel et al., 2001 ; Oh et al., 2001) have been studied the effect of ultrasonic waves in the liquid. Applying ultrasonic waves in a medium may cause the flow velocity of the medium to increase : an effect known as acoustic streaming (Frenkel et al., 2001). It has been reported that acoustic streaming promotes heat transfer through convection and affects the thermal boundary layer. Oh et al.(2001) have studied the relationship between melting with and without ultrasonic vibrations during the melting of a phase change material (PCM). They reported the acoustic enhancement of heat transfer in the liquid region. Judging from this, it is necessary to find out the relationship between the augmentation of heat transfer and the acoustic pressure distribution.

2. Experiments

Liquid paraffin (n-octadecane) with the boiling point of 300℃ was selected as a medium whose are listed in Table 1. Experiments were conducted in a melting cavity in Fig. 1(a) after the completion of the melting of solid paraffin. The melting cavity has an inner dimensions of 13 cm ×12.5 cm ×12.5 cm (height ×length × width). A stainless-steel plate heater was vertically positioned on the left side of the cavity, pro-

Table 1 Thermal properties of liquid paraffin

Properties	Value
Boiling Temperature	300℃
Thermal Conductivity	0.18 kcal/hr℃m
Density	863.03 kg/m^3
Specific Heat	686.54 kcal/kg℃
Viscosity	1.00 m^2/hr
Heat of Fusion	57.74 kJ/kg
Thermal Expansion Coefficient	0.001

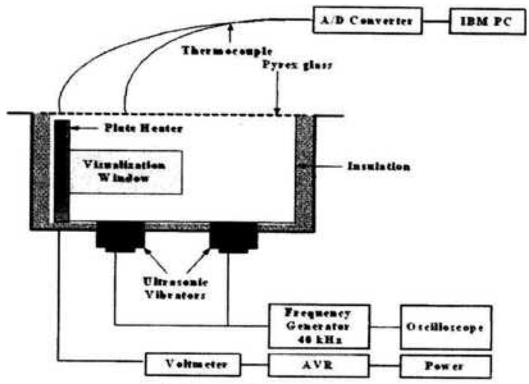

(a) Experimental set-up

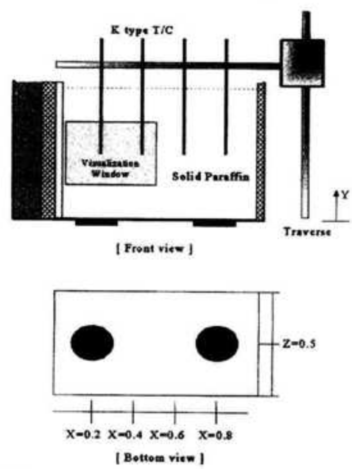

(b) Detail view of test section

Fig. 1 Schematic diagram of experimental set-up and test section viding a constant heat flux, $q''=6433.13\ W/m^2$ regulated by an automatic voltage regulator (AVR) during the melting process. Generally, the physical properties of the paraffin tend to change when temperature increases above 200℃ because the continuous chains of carbon atom are apt to break up at that temperature (Hong, 1990). Therefore, it is necessary to keep the heater temperature below 200℃. To achieve that, we used the heat flux of $6433.13\ W/m^2$ under which the heater surface temperature was kept below 200℃. To obtain a constant heat flux boundary condition, a plate heater was heated electrically by an automatic voltage regulator (Powertek, PAV-500) which was designed to maintain a constant output voltage within ±1% of nominal, with an input voltage variation of ±20%. The back of the heater surface was insulated with a bakelite plate and fiberglass so that the heat flux would propagates only to the forward direction from the heater surface. Also, all four outside walls of the cavity were covered with styrofoam and fiberglass plate for insulation purpose. The resonance frequency of 40 kHz was applied from the frequency generator to two ultrasonic transducers. All thermocouples were connected to a data acquisition controller. The temperatures at different positions were automatically recorded at a PC.

Two ultrasonic transducers are installed at two axial locations (i.e., $X=0.2$ and $X=0.8$) as shown in Fig. 1(b). Four chromel-alumel thermocouples of 15 cm length were installed at pre-selected locations ($X=0.2$, 0.4, 0.6, 0.8 and $Z=0.5$) by using a traverse which can be controlled the accurate position to 0.5 mm in order to measure the temperature distribution during the melting process in the melting cavity. Each thermocouple was wound in an insulation tape and was sheathed in a stainless-steel tube except at the junction to minimize heat conduction from a connecting thermocouple wire to the liquid. Before the experiments, all thermocouples were calibrated with a calibration voltage source. The melting was carried out three times under the same condition in order to obtain the accurate temperature distribution for each experimental case. The largest temperature deviations from the average temperature were about ±5℃ (i.e., ±3.3 %) on the heater, and about ±2℃ (i.e., ±2.4%) in the paraffin. In the present study, a particle image velocimetry (PIV) was used for the visualization of flow field inside the liquid region of the paraffin. Although a fixed frequency level of 40 kHz was selected, ultrasonic intensities were varied from 70 W to 340 W in order to investigate the effect of the ultrasonic vibrations strength on heat transfer.

3. Numerical Analysis

The acoustic pressure distribution in a liquid can be experimentally obtained by a hydrophone. However, it is impossible to obtain the reliable pressure value with a hydrophone when the liquid is heated over 120℃. As discussed, in the present study, the liquid paraffin in a cavity was heated over 135℃ under a constant heat flux condition. Hence, numerical analysis was applied to calculate the acoustic pressure in the liquid paraffin, instead of experimental measurements. For numerical analysis, SVS[1] (Structure Vibration Simulator) programmed with Fortran language and based on a coupled FE-BEM was used. In recent years, researchers (McCollum and Clementina, 1996 ; Jarng, 1998) have developed the theory of a coupled FE-BEM which is designed to solve a vibrating problem in an infinite space. Not only this technique can reduce the time of the modeling but also the acoustic pressure and noise prediction in an infinity boundary can be possible.

Figure 2 displays a finite element, a finite mesh and a fixed boundary of a vibrating plate. The vibrating plate composed of 203 elements and 1534 nodes was re-meshed to follow the mesh arrangement of SVS after the mesh generation of ANSYS™. Each element is composed of 20 quadratic nodes and each surface boundary has 8 quadratic nodes. The element size of the numerical model does not exceed about 4.2 mm, which is about 1/6 of the wavelength of 40 kHz waves in

[1] SVS is a commercial FE-BEM package which was developed and programmed by Dr. Jarng, who is a professor of Chosun University.

the liquid paraffin in order to assure the accuracy of the numerical analysis. In addition, as shown in Fig. 2(c), all elements are fixed except two ultrasonic transducers where a high frequency vibration of the excited plate radiates ultrasonic waves to the liquid paraffin.

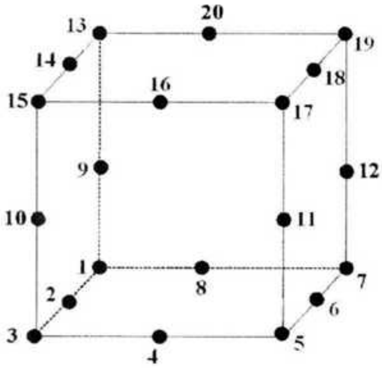

(a) Element of composed 20 quadratic nodes

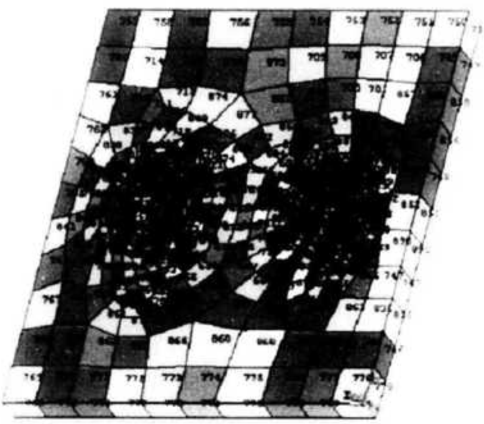

(b) Finite-element meshes for a vibrating plate

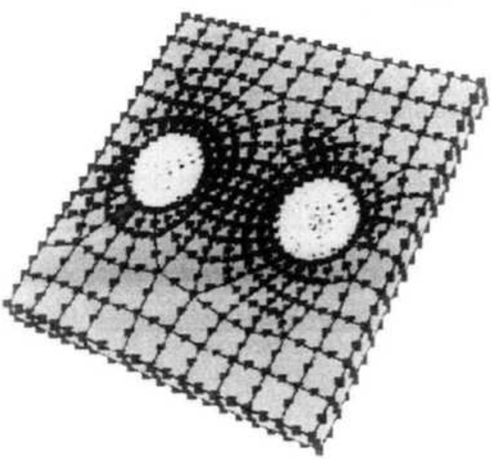

(c) Fixed boundary condition for a vibrating plate

Fig. 2 Numerical modeling for a coupled FE-BEM

4. Results and Discussions

4.1 PIV measurements

The PIV observation clearly shows that the application of the ultrasonic vibrations to the liquid initiates a strong upward flow, acoustic streaming. In general, acoustic streaming can be classified into two types. The first, which has received the majority of attention to date, is Rayleigh streaming. This is caused by relative oscillatory motion between the fluid and a boundary. The steady flow results from the rapid change in the wave amplitude in the acoustic boundary layer. The effects of attenuation are

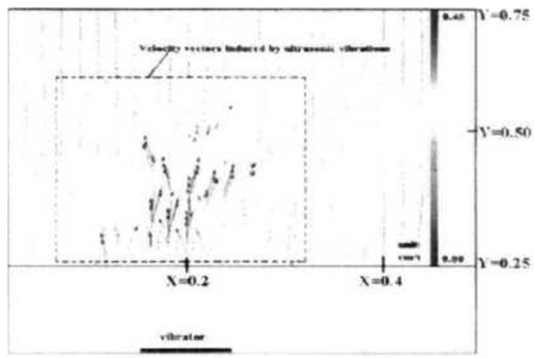

(a) Velocity profiles calculated from the PIV

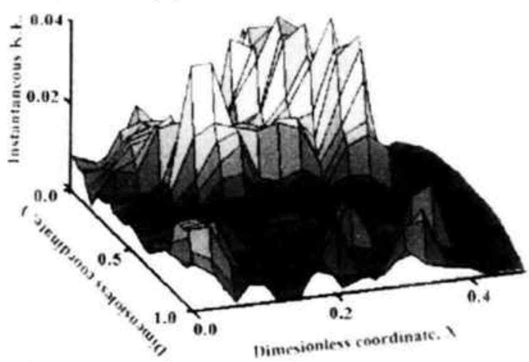

(b) Kinetic energy distribution calculated from the PIV

Fig. 3 Two dimensional velocity profiles and kinetic energy distribution induced by ultrasonic wave measured at the visualization window at the output power level of 340 W

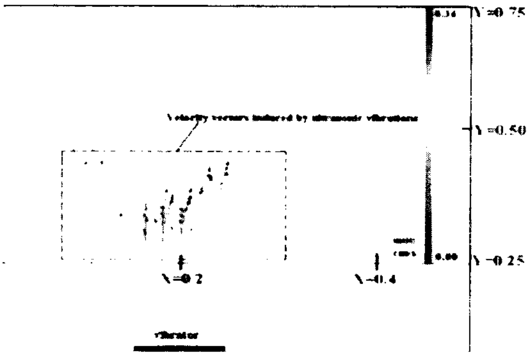

(a) Velocity profiles calculated from the PIV

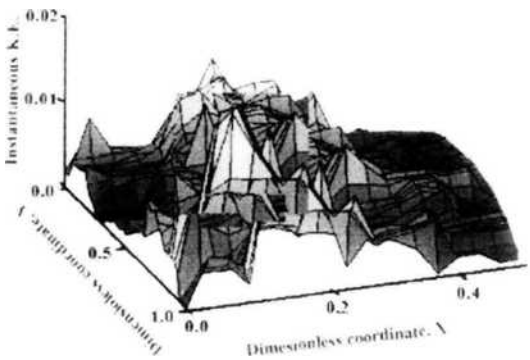

(b) Kinetic energy distribution calculated from the PIV

Fig. 4 Two dimensional velocity profiles and kinetic energy distribution induced by ultrasonic wave measured at the visualization window at the output power level of 185 W

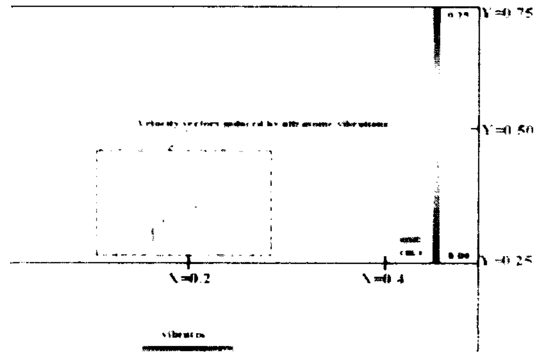

(a) Velocity profiles calculated from the PIV

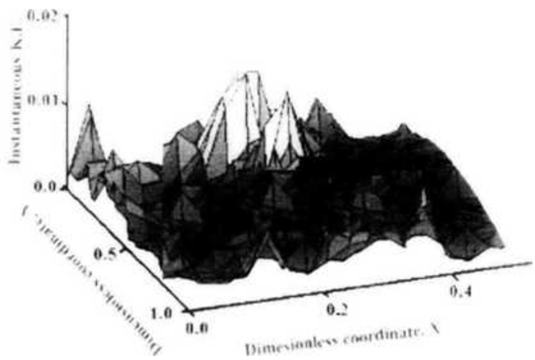

(b) Kinetic energy distribution calculated from the PIV

Fig. 5 Two dimensional velocity profiles and kinetic energy distribution induced by ultrasonic wave measured at the visualization window at the output power level of 70 W

usually considered to be negligible. The second, Eckart streaming, results from the attenuation of the wave in the bulk fluid. Here the momentum transfer from the wave is converted into a time-averaged flow moving away from the source (Haydock and Yeomans, 2001). According to the above classification, the acoustic streaming observed in the present study is close to quasi-Eckart streaming which can generate an intense fluid motion. This flow seems to increase heat and mass transfer, destroying the flow instability.

In the present study, three different output power levels (70 W, 185 W and 340 W) at a frequency generator were adjusted to investigate the effect of ultrasonic intensity on heat transfer. As shown in Figs. 3~5, the upward flow initiated from the point where the ultrasonic transducer is attached (i.e., dimensionless coordinate X= 0.2) becomes intense as the ultrasonic intensity varies from 70 W to 340 W. Consequently, this intense flow motion results in the higher kinetic energy distribution at the same location.

4.2 Augmentation ratio of heat transfer

In order to examine the heat transfer behavior, the Nusselt number divided by $Ra^{*0.25}$ (defined in Eq. (1)) was plotted in Fig. 6 against normalized time, τ for two different experimental conditions (i.e., the case without ultrasonic vibrations and the other with ultrasonic vibrations) during the whole melting process.

$$Nu/Ra^{*0.25} = \frac{q''H}{\Delta TK} \Big/ \left(\frac{g\beta q'' H^4 \mathrm{Pr}}{k\nu^2} \right)^{0.25} \quad (1)$$

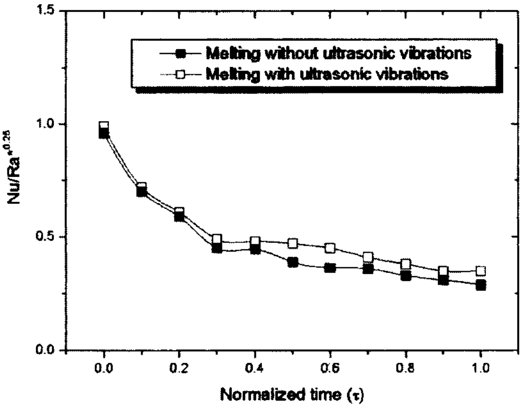

Fig. 6 Nusselt number variation against normalized time (τ) at the output power level of 185 W

Where, ΔT is the temperature difference between heater surface and paraffin. The normalized time was obtained by dividing time by the total time consumed to melt the solid paraffin completely. The power of 0.25 over Ra* was generally used in the natural convection problem (Hong, 1988). As shown in Fig. 6, after normalized time, $\tau=0.3$, the heat transfer coefficient is increased by about 12%~19% when the ultrasonic vibration was applied. Figure. 6 clearly illustrates that applying ultrasonic vibrations into a liquid can increase the heat transfer coefficient during the melting process. Increase in the heat transfer coefficient is due to the fluid dynamic motions which largely depend on acoustic streaming. Judging from this, it is required to relate the acoustic pressure which can initiate acoustic streaming to the heat transfer behavior in the liquid region. Therefore, in the present, the heat transfer behavior in the liquid paraffin was investigated in terms of local heat transfer coefficient after the completion of melting, as mentioned. Local heat transfer coefficient in the liquid can be calculated from:

$$h=\frac{q''}{T_h-T_\infty(x,\ y,\ t)} \tag{2}$$

where, q'' is the heat flux, T_h is the heater surface temperature and T_∞ $(x,\ y,\ t)$ is the liquid temperature of selected location. The augmentation ratio of heat transfer (Δh) in the liquid is defined as following:

$$\Delta h=\frac{h}{h_0} \tag{3}$$

where, h and h_0 are the heat transfer coefficient with and without ultrasonic vibrations, respectively.

4.3 Acoustic pressure distribution in the liquid

Acoustic pressure $p(r,\ t)$ caused by the wave propagation in a non-viscous compressible fluid is governed by the following wave equation.

$$\nabla^2 p-\frac{1}{c^2}\frac{\partial^2 p}{\partial t^2}=0 \tag{4}$$

Where, r and t are the space and time coordinates, respectively. ∇^2 is Laplacian. The velocity of vibrating plate surface was calculated from the vibrating displacement obtained by the FEM and then was considered as the boundary condition for the BEM. The reflection of ultrasonic waves from the free surface or the cavity wall is neglected.

To calculate pressure using the BEM, the wave speed in a medium should be determined. In general, the wave speed and density in a medium are proportional to the temperature of a medium. In the present study, the temperature of the liquid paraffin was determined from the following equation (Hong, 1990; Mashiro, 1995):

$$T_{avg}=\frac{1}{2}(T_h+T_\infty) \tag{5}$$

For the density estimation, the following relation which a paraffin manufacturer, *Shinyo Pure Chemical Co* provided was used:

$$\rho=778.3\exp[-8.249\times10^{-4}(T-50)] \tag{6}$$

The wave velocity, ν in a medium was obtained by relating the results from Eqs. (5) and (6) to the following equation:

$$\nu=\sqrt{\frac{E}{\rho}}=\sqrt{\frac{1}{k_T\rho}} \tag{7}$$

Where, E is bulk modulus and k_T is compressibility. The Bulk modulus of the liquid paraffin between 1atm and 100atm listed in Table 2 come from CRC handbook of chemistry and physics (Cutler et al., 1958).

Table 2 Bulk modulus of elasticity of paraffin (n-octadecane)

Temperature	Bulk modulus of elasticity (N/m^2)	
	1 atm	100 atm
60.0	1.06×10^9	1.96×10^9
79.4	9.61×10^8	1.82×10^9
98.9	8.62×10^8	1.72×10^9
115.0	7.81×10^8	1.64×10^9
135.0	6.94×10^8	1.56×10^9

4.4 Comparison between experimental and numerical results

In Figs. 7~9, the acoustic pressure predicted by numerical analysis was compared with the augmentation of heat transfer experimentally measured under three different ultrasonic intensities. As shown in Figs. 7(a)~9(a), the acoustic pressure is higher at the points where two ultrasonic transducers (i.e., X=0.2 and X=0.8) are installed than other points. Especially, at the dimensionless coordinate, Y=0.25 and X=0.2 and X=0.8, the acoustic pressure experiences the maximum value for all different ultrasonic intensities. These points are in a good agreement with points where the kinetic energy distribution is higher (see Figs. 3~5). However, in case of Y>0.25, there is no large deviation in the acoustic pressure because acoustic waves uniformly propagate through the whole liquid region as shown in Fig. 10. A similar observation was reported by Kim et al. (1995). The acoustic wave emitted from the transducers travels throughout the enclosure

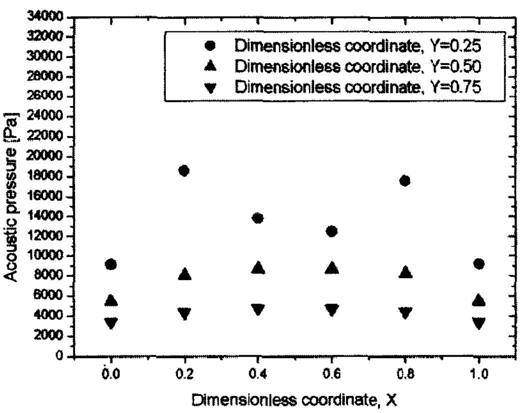

(a) Acoustic pressure variations

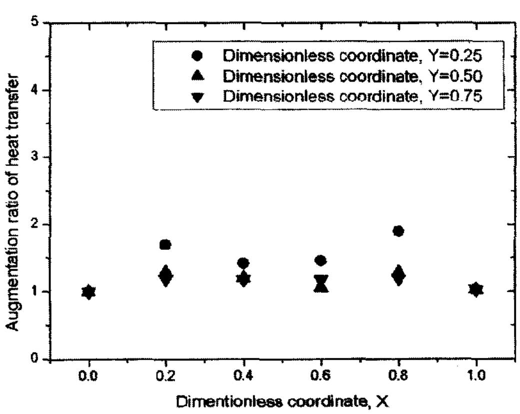

(b) Augmentation ratio of local heat transfer

Fig. 7 Comparison between the acoustic pressure distribution and augmentation ratio of heat transfer at the ultrasonic intensity of 340 W

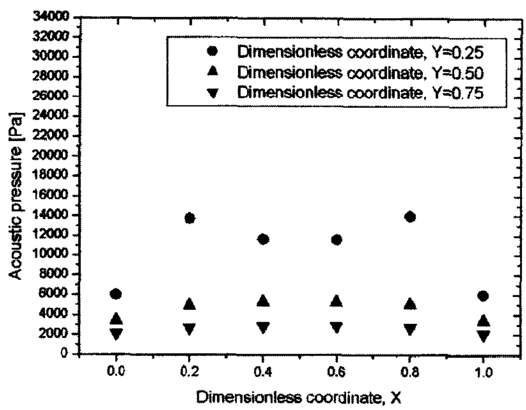

(a) Acoustic pressure variations

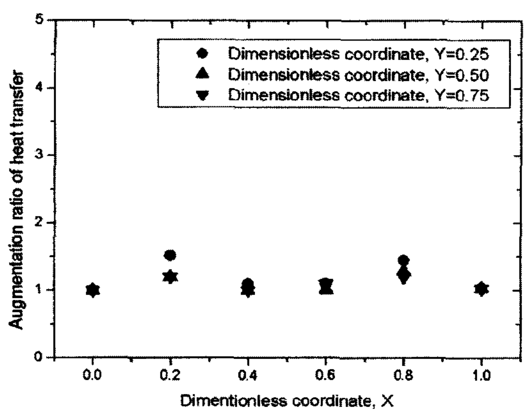

(b) Augmentation ratio of local heat transfer

Fig. 8 Comparison between the acoustic pressure distribution and augmentation ratio of heat transfer at the ultrasonic intensity of 185 W and creates waves of compression and expansion in the liquid which result in acoustic pressure variations. As a result, a strong upward flow, called Eckart streaming starts to develop at the same time that the kinetic energy increases.

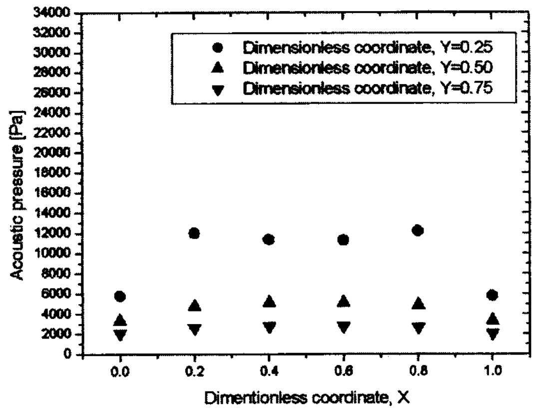

(a) Acoustic pressure variations

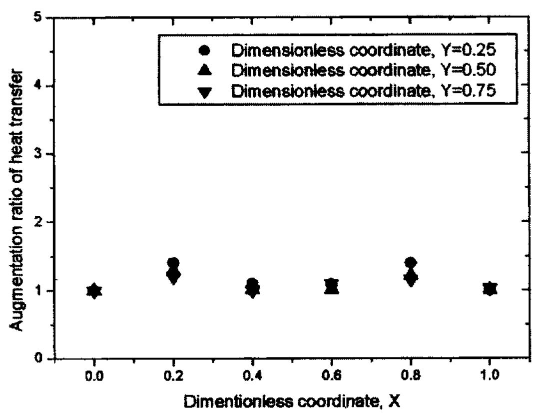

(b) Augmentation ratio of local heat transfer

Fig. 9 Comparison between the acoustic pressure distribution and augmentation ratio of heat transfer at the ultrasonic intensity of 70 W

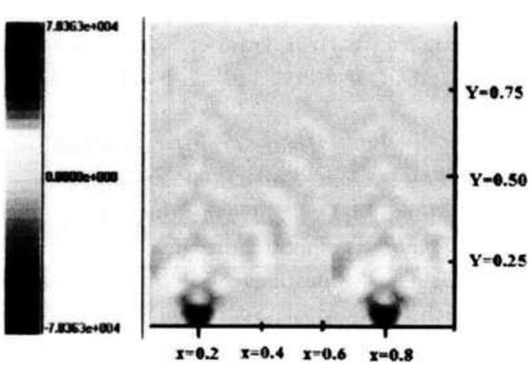

Fig. 10 Two dimensional acoustic pressure distribution calculated by a coupled FE-BEM

The augmentation ratio of heat transfer was plotted in Figs. 7(b)~9(b), respectively. It is also higher at the points where two transducers are attached because the strong ultrasonic waves cause the flow velocity of the liquid to increase and promote heat transfer as revealed in the PIV measurement. Even though the profiles between the acoustic pressure and heat transfer augmentation are not exactly matched for each other, they still have a similar pattern. In Table 3, the calculated acoustic pressure and the augmentation ratio of heat transfer for three different ultrasonic intensities are listed with respect to dimensionless coordinates. As tabulated in Table 3, an increase in the acoustic pressure can enhance the ratio of heat transfer. From these results, one can conclude that acoustic pressure induced by ultrasonic waves initiates an intense flow motion such as Eckart streaming which helps to increase the local heat transfer.

Table 3 Acoustic pressure and the augmentation ratio of heat transfer for three different ultrasonic intensities

Power [W]	X	Augmentation ratio of heat transfer			Acoustic pressure [Pa]		
		Y=0.25	Y=0.50	Y=0.75	Y=0.25	Y=0.50	Y=0.75
340	0.0	0.998	0.998	0.998	9,137	5,453	3,413
	0.2	1.700	1.285	1.188	18,579	8,058	4,355
	0.4	1.412	1.199	1.176	13,789	8,690	4,756
	0.6	1.453	1.056	1.179	12,505	8,667	4,708
	0.8	1.898	1.284	1.193	17,582	8,264	4,446
	1.0	1.035	1.029	1.028	9,217	5,484	3,427
185	0.0	0.998	0.998	0.998	5,985	3,408	2,111
	0.2	1.510	1.199	1.201	13,735	4,924	2,677
	0.4	1.100	1.005	1.001	11,665	5,298	2,884
	0.6	1.099	1.007	1.098	11,618	5,305	2,888
	0.8	1.444	1.284	1.199	13,988	5,041	2,727
	1.0	1.035	1.029	1.028	5,994	3,410	2,112
70	0.0	0.998	1.002	0.998	5,782	3,298	2,044
	0.2	1.400	1.280	1.200	12,000	4,779	2,594
	0.4	1.098	1.005	1.001	11,361	5,146	2,797
	0.6	1.089	1.007	1.098	11,279	5,149	2,800
	0.8	1.395	1.208	1.156	12,201	4,891	2,644
	1.0	1.001	1,000	1.028	5,783	3,299	2,045

5. Conclusions

The augmentation ratios of heat transfer coefficient were experimentally measured and were compared with the profile of acoustic pressure obtained by numerical prediction when the ultrasonic waves were applied in the liquid paraffin. The present study provides a significant evidence that a strong fluid motion initiated by ultrasonic waves can affect heat and mass transfer. This phenomenon, called acoustic streaming, clearly observed by the PIV measurement leads to increase in the velocity and the kinetic energy of a fluid which is a crucial physical concept to explain the enhancement of convective heat transfer. The heat transfer coefficient is increased with increase in the ultrasonic intensities. The largest augmentation of heat transfer (about 28%) is measured at the ultrasonic intensity of 340 W. Acoustic streaming results from sudden acoustic pressure variations in the liquid. The results of numerical analysis show acoustic pressure is increased by 60.3%, 39%, and 35% at the ultrasonic intensity of 340 W, 185 W and 70 W, respectively. The higher acoustic pressure distribution near two ultrasonic transducers develops more intensive flow (quasi-Eckart streaming), destroying the flow instability. Also, the profile of acoustic pressure variation is consistent with that of augmentation of heat transfer. This mechanism is believed to increase the ratio of heat transfer coefficient.

Acknowledgment

This study was supported in part by a research fund from Chosun University 2003.

References

Cutler, W. G., McMickle, R. H., Webb, W. and Schiessler, R. W., 1958, *J. Chem. Phys.*, Vol. 29, p. 727.

Frenkel, V., Gurka, L. and Shavit, U., 2001, "Preliminary Investigations of Ultrasonic Induced Acoustic Streaming Using Particle Image Velocimetry," *Ultrasonics*, Vol. 39, pp. 153～156.

Fsairbanks, H. V., 1979, "Influence of Ultrasound upon Heat Transfer Systems," *Ultrasonics Symposium*, pp. 384～389.

Haydock, D. and Yeomans, J. M., 2001, "Lattice Boltzmann Simulations of Acoustic Streaming," *J. Phys. A, Math. Gen*, Vol. 34, pp. 5201～5213.

Hong, C. S., 1990," Studied on Heat Storing and Retrieving Characteristics in a Paraffin-Filled Horizontal Circular Tube," Ph. D. Thesis, University of Seoul, Seoul, Korea.

Hong, J. S., 1988, "Experimental Study of Melting Phenomena with and without ultrasonic vibrations," M. S. Thesis, University of Illinois, Chicago, Illinois.

Iida, Y., Tsutsui, K., Ishii, R. and Yamada, Y., 1991, "Natural Convection Heat Transfer in a Field of Ultrasonic Waves and Sound Pressure," *Journal of Chemical Engineering of Japan*, Vol. 24, pp. 794～796.

Jarng, S. S., 1997, "Sonar Transducer Analysis Using a Coupled FE-BE Method," *Proc. of the 12 Korea Automatic Control Conf.*, Vol. 12, pp. 1750～1753.

Kim, J. O., Kim, J. H., Choi, J. Y. and Jho, M. J., 1995," A Study on Improving the Life and Performance of an Ultrasonic Cleaner by Vibration and Acoustic Analyses," *Journal of KSME*, Vol. 19, No. 11, pp. 2939～2953.

Larson, M. B. and London, A. L., 1962," A Study of the Effect of Ultimate Vibrations on Convective Heat Transfer to Liquids," *ASME*, 62-HT-44, pp. 62～68.

Lemlich, R., 1955, "Effect of Vibration on Natural Convective Heat Transfer," *Industrial and Engineering Chemistry*, Vol. 47, No. 6, pp. 121～127.

Mashiro, 1995, *Heat Transfer, Korean ed., Sigma Press, Seoul, Korea*, 200-2001.

McCollum, M. D. and Clementina, M. S., 1996, "Modal Analysis of a Structure in a Compressible Fluid Using a Finite Element/Boundary Element Approach," *J. Acoust. Soc.* Am. 99, pp. 1949～1957.

Oh, Y. K., Park, S. H. and Cha, K. O., 2001, "An Experimental Study of Accelerating Phase

Change Heat Transfer," *KSME International Journal*, Vol. 15, pp. 1882~1891.

Topp, M. N. and Eisenklam, P., 1972, "Industrial and Medical Uses of Ultrasonic Atomizers," *Ultrasonics*, pp. 127~132.

West, F. B. and Taylor, A. T., 1952, "The Effect of Pulsations on Heat Transfer," *Chem. Eng. Progress.*, Vol. 48, No. 1, pp. 208~214.